16th Australasian Fluid Mechanics Conference
Crown Plaza, Gold Coast, Australia
2-7 December 2007

Modelling tsunami inundation on coastlines with characteristic form

**T. E. Baldock[1], M. P. Barnes[1], P. A. Guard[1], Thomas Hie[1],
D. Hanslow[2], R. Ranasinghe[2], D. Gray[3], O. Nielsen[3]**

[1]Coastal Engineering Research Centre, Div. Civil Engineering

University of Queensland, St Lucia, QLD407, AUSTRALIA

[2]NSW Department of Natural Resources, PO Box 2185, Dangar, NSW 2309, AUSTRALIA.

[3] Geoscience Australia, GPO Box 378, Canberra, ACT 2601, AUSTRALIA

Abstract

This paper provides an indication of the likely difference in tsunami amplification and dissipation between different characteristic coastal embayments, coastal entrances and estuaries. Numerical modeling is performed with the ANU/Geoscience Australia tsunami inundation model. Characteristic coastal morphology is represented by simpler generic morphological shapes which can be applied easily in the ANUGA model, such that key non-dimensional parameters (e.g. embayment depth/bay width) can be varied. Modeling is performed with a range of bay shapes, seabed gradient and different incident tsunami wave shapes and wave angles, including sine waves, solitary waves and leading depression N-waves. The results show a complex pattern for both large and small embayments, with wave breaking an important control on the amplification of the wave between the 20m contour and the shore. For large embayments, the wave run-up can be amplified by a factor six in comparison to the amplitude at the model boundary. For small embayments, the amplification is dependent on the location of the ocean water line, or tidal stage.

Introduction Australian coastal communities face the relatively low-level, but nevertheless real, threat of severe natural flooding and overtopping of coastal barriers due to tsunami. Tsunamis are typically generated by offshore earthquakes, with active regions close to Australia including the Java Trench, the Solomon Trench, and the Puysegur Ridge to the Northwest, Northeast, and Southeast respectively. Landslides on the continental slope also have the potential to generate tsunami waves propagating both offshore and onshore. As demonstrated by the 26 December 2004 Asian tsunami, inundation and resulting devastation are significantly related to localised effects. Tsunami waves are refracted, diffracted, reflected and amplified during propagation through shallow water.

The bathymetry has a strong influence on the resulting runup and shoreline inundation. In particular, for the same offshore incident tsunami waves, very different inundation patterns are expected between open coasts, bays and estuaries. However, at present, the magnitude, direction and shape of incident tsunami waves are uncertain and cannot be defined in terms of usual risk assessment parameters. Consequently, detailed tsunami modelling using specified tsunami wave shapes is not possible in order to perform risk assessments and it is difficult to determine the exact level of risk. Nevertheless, some method of identifying sites that are most vulnerable to tsunami hazard is required.

This paper presents results forming a basis for identifying sites along the NSW coastline that are most vulnerable to tsunami inundation. Typical representative coastal morphology are identified and represented by simple generic shapes for modelling purposes. Localised inundation effects due to coastal bay morphology including length, breadth, orientation, entrance width, and depth are explored. Three theoretical tsunami wave shapes are modelled for various wave angles and for both breaking and non-breaking cases. Two scales of coastal morphology are considered – small scale embayments, of order 400-500m length and breadth, and large scale embayments, of order 5km length and breadth. The modelling is performed with the ANUGA Hydrodynamic model (Nielsen et al., 2005) which is public domain software provided by Geoscience Australia.

This paper is organised as follows. The remainder of section 1 presents a brief outline of the ANUGA model. Some background theory on tsunami waves that is relevant to the study is also presented. Section 2 outlines the study methodology, the bay configuration, the tsunami wave conditions and presents tables of the combinations of wave shape and bay configurations that have been investigated. Results for small embayments (order 1km length and width) are presented in Section 3. Section 4 presents results for large bays (order 5 km length and width). Conclusions follow in Section 5, with recommendations for further research in Section 6.

Tsunami Wave Shapes and Analytical Solutions

The shape of an incoming tsunami wave profile depends on the nature of the generation source (e.g. slow-moving landslide, abrupt seabed rupture) and the bathymetry over which it has propagated. Thus the likely wave profile at a given location is difficult to predict and will be highly dependent on the details of the seafloor movement in the generation region. For the purposes of this study, three incident tsunami wave profiles were adopted: a sine wave, a solitary wave and an N-wave. To be consistent with the existing literature, and to enable comparison with analytical results, the solitary wave and N-wave profiles suggested by Synolakis (2003) were used. The sine wave was included to allow comparison with the non-breaking analytical solutions of Carrier and Greenspan (1958).

Carrier and Greenspan (1958) presented solutions for wave run-up on a plane beach for the case where the waves do not break. Keller and Keller (1965) show that the amplification ratio for the run-up compared to the wave height based on linear theory is given by

$$\frac{R}{A} = \left(J_0^{\,2}\left(\frac{2\sqrt{kh_0}}{\beta} \right) + J_1^{\,2}\left(\frac{2\sqrt{kh_0}}{\beta} \right) \right)^{-\frac{1}{2}} \quad (1)$$

where R is the run-up elevation and A and k are the wave amplitude and wave number at offshore depth h_0. For large arguments ($kh_0 > 1$) the amplification ratio (1) can be simplified to

$$\frac{R}{A} = \sqrt{\frac{\pi}{\beta}} \left(kh_0 \right)^{\frac{1}{4}} \qquad (2)$$

This result is valid for both the linear and non-linear standing wave solutions. Lamb (1932) also provides a periodic standing wave solution for the case of a V-shaped bay where the still water line is located at the apex of the bay. In this case the amplification ratio given by

$$\frac{R}{A} = \sqrt{\frac{\pi}{\beta}} \left(kh_0 \right)^{\frac{3}{4}} \qquad (3)$$

Figure 1 shows the shape of the Bessel function standing wave profiles and the envelope functions used as the basis for equations (1), (2) and (3).
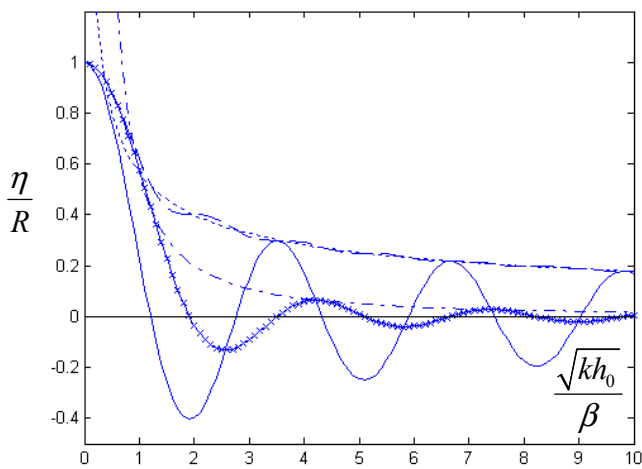

Figure 1. The standing wave profile on a plane beach (line) and in a V-shape bay (line with crosses). The envelope functions used to derive equations (1) (dashed), (2) (dotted) and (3) (dot-dashed) are also shown.

Synolakis (1987, 2003) uses the same transformation of the equations and a semi-analytic contour integration method to arrive at the solution for the run-up of solitary waves and N-waves. The results corresponding to equation (1) are

Solitary wave run-up: $\quad \frac{R}{A} = 2.831 \sqrt{\frac{1}{\beta}} \left(p_0 \right)^{\frac{1}{4}} \left(\frac{A}{h_0} \right)^{\frac{1}{4}} \qquad (4)$

Leading depression N-wave run-up:

$$\frac{R}{A} = 5.48 \sqrt{\frac{1}{\beta}} \left(p_0 \right)^{\frac{1}{4}} \left(\frac{A}{h_0} \right)^{\frac{1}{4}} \qquad (5)$$

Here, the amplification is relative to a wave amplitude A at an offshore location where the depth is h_0. For very small beach slopes, it is expected that a breaking criteria limits the validity of the non-breaking wave solutions. In addition, all the analytical solutions are for inviscid flow. This suggests that they are likely to overestimate the run-up, which consists of a thin tip in the analytical solutions. Guard et al. (2005) presented solutions for run-up from breaking tsunami waves, but only for plane beaches.

Methodology
The coastal morphology along the NSW coast varies from open (plane) beaches to a variety of embayment shapes. Tsunami inundation patterns are governed by the shelf bathymetry, nearshore bathymetry and beach bathymetry, as well as wave shape, wave angle and wave frequency. For any particular coastal location, likely tsunami wave characteristics are at present largely unknown. Consequently, assessing detailed tsunami hazards at any particular requires a full ocean tsunami model initiated by an appropriate source, coupled to a nearshore tsunami model using

detailed local bathymetry. At present, this is not practical along the full coastline. This study adopts a different approach and seeks to identify the effects of different geomorphology on tsunami run-up and penetration. The run-up of typical tsunami waves for different characteristic (generic) coastal geomorphology is investigated and compared to the run-up on plane beaches, representing open coasts. This provides a measure of the additional hazard, or risk, that might be expected at different locations for a given incident tsunami wave.

Examples of different coastal geomorphology include box shape, rectangular or square bays, V-shape or triangular bays, U-shaped or circular bays, and combinations of the above. The width to length ratio of typical embayments along the NSW coast ranges from W/L=0.5-4, with larger values representing more open bays and smaller numbers representing narrow, deeper bays. The purpose of the present study is to compare tsunami run-up penetration for generic morphology of these forms to the run-up obtained on a plane beach. For the plane beach, straight parallel contours represent a reasonable approximation, and consequently, straight parallel contours are adopted for the generic bay shapes. While the latter is an approximation, it allows for consistent comparison between the results for open coasts and bays.

Generic Bay Shapes
Figures 2 illustrates the three generic bay shapes used in the study Each bay shape was defined by the long-shore width, W, and the cross-shore length, L. Three ratios of W/L were investigated: 0.5, 1, and 2. Figure 2.2 presents typical contour plots of bed elevation for each bay shape. In all cases, the bed slopes were set to a linear slope. Vertical walls form the bay and are simply represented in ANUGA as reflective boundaries. The same linear profile is set seaward of the bay entrance. For each bay shape the seaward extent is limited to the -20 m contour line. The 0 m contour line represents the still water line (SWL) position.
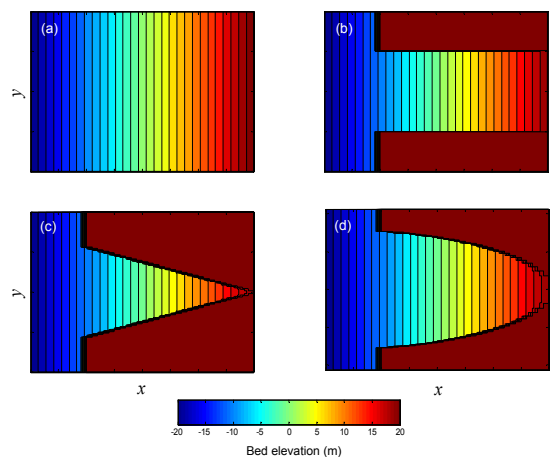

Figure 2. Typical bed elevation (m) contour plots for three generic bay shapes: (a) plane beach (b) rectangular bay; (c) triangular bay; (d) circular bay.

Two scales of embayment are considered. Small bays (L_B=400 m) are representative of the many small embayments along the NSW central coast in particular. For the results presented here, the ocean still water level is set at the quarter point of the bay to ensure run-up does not reach the landward limit. This is to ensure all the run-up occurs over the sloping beach. Large bays (L_B=5000 m) are representative of larger coastal morphology and estuarine systems. In this case, the ocean still water level is set at the landward limit of the bay, since at this scale beaches at the landward end represent a very small fraction of the total bay

length. The maximum inundation level is taken as the maximum water level observed at the apex of the bay. For the small embayments, the same beach slope is maintained as for the plane beaches (1:10 to 1:50). For the large bays, the bathymetry within the bay is set to a linear slope between the apex of the bay and the offshore boundary. This corresponds to a slope of 20 m/7000 m, or 1/350, similar to that of Batemans Bay, for example.

Tsunami wave conditions

Since the tsunami sources for the NSW coastline remain uncertain, the tsunami wave conditions near the coastline are not well specified, in terms of direction, wave height and wave period, as well as wave shape. Therefore, three wave shapes are considered, sine waves, solitary waves and N-waves, each for a range of wave heights or wave steepness, wave period and wave angle. The model runs are initiated in a water depth of d=20m. Run-up and tsunami wave penetration are referenced to the specified wave amplitude at this water depth. For the sine waves and N waves, the wave amplitude (A=H/2) represents the maximum ocean elevation for the incident wave. For the solitary wave, H represents the maximum ocean level above the still water condition. It is assumed that ocean propagation models will provide incident tsunami conditions at this water depth in for the purposes of later risk assessments. A range of wave periods and wave amplitudes (or wave steepness) was used for each wave type, giving both non-breaking and breaking waves.

Results
Small bays

Amplification ratios for sine waves incident on plane beaches and small bays are shown in figures 3 &4 . The amplification ratio is plotted versus both wave period and a non-dimensional parameter derived from the Carrier and Greenspan (1958) solution which describes the width of the shoaling zone, χ. This parameter can be written as

$$\chi = \sqrt{\frac{\pi}{\zeta_0}}\left(\frac{2\pi}{H_0/d_0}\right)^{\frac{1}{4}} \text{ or } \chi = \sqrt{\frac{\pi}{\beta}}(k_0 d_0)^{\frac{1}{4}} \quad (6)$$

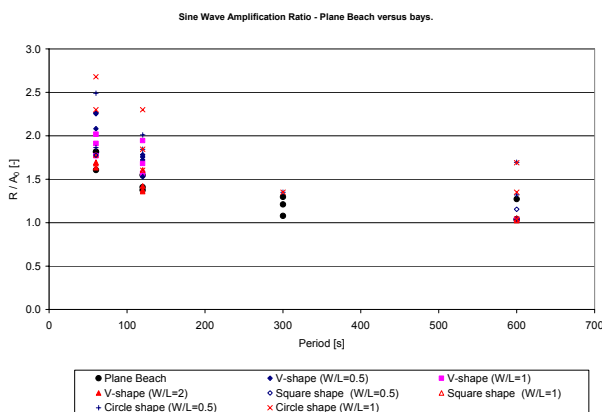where ζ_0 is the Iribarren number ($\zeta=\beta/\sqrt{(H_0/L_0)}$).

Figure 3. Sine wave amplification. Plane beach versus bay. Beach slope=0.1.

The modelling demonstrates a clear frequency sensitivity. For sine waves of 600s and over, very little amplification occurs between the offshore boundary of the model (20m water depth) and the shoreline. This is consistent with very long waves flooding up to the offshore water level. Significant amplification (greater than 1.5) only occurs for periods less than about 300s, or 5 minutes. While tsunami waves are generally assumed to be long period waves of order 20 minutes or more, these shorter period waves frequently occur at the front of tsunami as the wave breaks up over the shelf. Short period leading waves, frequently breaking, were also observed in the 2004 Indian Ocean tsunami.
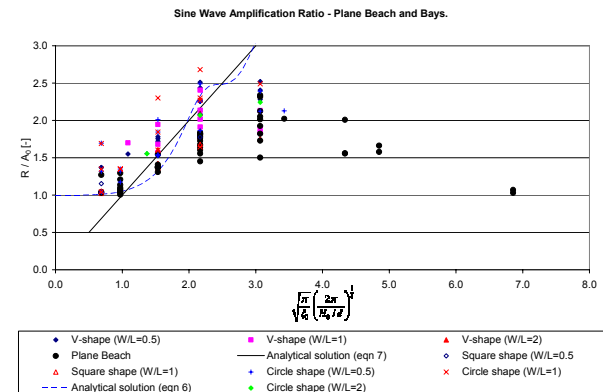

Figure 4. Sine wave amplification. Plane beach versus bay.

Maximum amplification for the shorter period sine waves occurs with for value of χ between 2 and 3, before wave breaking reduces the maximum amplification. For long period tsunami waves (or steep beaches), the model results approach the analytical solution and shows the same trend with non-dimensional shoaling distance. The influence of bay shape is significant, again predominantly for shorter period waves. In general, the narrower the bay (smaller W/L) then greater amplification occurs, but this can again be influenced by wave breaking and the complete behaviour is more complicated. The V-shape increases the maximum amplification from about 1.5 to 2.5. The influence of the V-shape is greatest for shorter wave periods, with the narrower bays giving an increase in the run-up amplification over the plane beach from 1.5 to 2.5, or 50%. Thus the bay can have a similar influence on the amplification to that of shoaling from the 20m contour to the shoreline, which is typically of order 50%. This is significant.

Results for solitary waves are shown in figure 5, using the non-dimensional beach slope derived by Synolakis (1987) to collapse the results for different beach slopes and wave steepness. The model results follow the expected trend for longer period waves or large beach slopes, and then show considerable scatter as breaking commences. The largest amplification occurs for waves just on the point of breaking at the shoreline. The bays typically appear to amplify solitary wave run-up by about 20%, but increases of 50% also occur. The V-shape bays result in much greater amplification than the square bays or circular bays, as expected from the geometry of the system. In particular, a relatively narrow (W/L=0.5) circular shaped bay with a beach gradient equal to 0.1 does not result in a significant increase in the run-up in comparison to a plane beach.

For the cases considered here, ANUGA predicts greater amplification for leading depression N-waves than for solitary waves which is consistent with theory. The effect of the bay shape is not significant except for small wave periods, which do not probably occur in the form of leading depression N-waves Nevertheless, for these periods, the run-up in the bays increases by up to 50%. The results for different beach slopes and wave conditions can again be combined using the Synolakis scaling (figure 6). Maximum amplification occurs at smaller values of the scaling parameter than for solitary waves, and with amplification ratios up to about 3.5. The model results appear to underestimate the theoretical solutions, which may be a combination of friction effects and numerical dissipation. However, of most interest here is the relative run-up between plane beaches and bays.

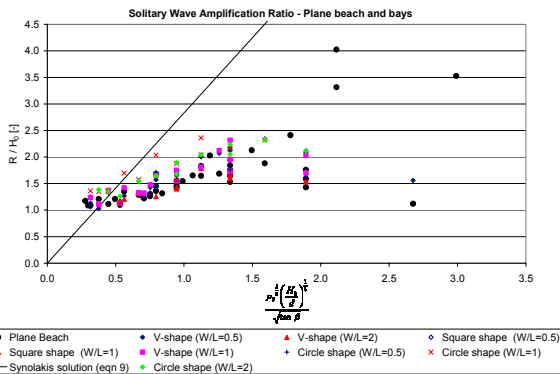**Solitary Wave Amplification Ratio - Plane beach and bays**

Figure 5. Solitary wave amplification.

For tsunami waves at an angle, the longshore length of the model domain was increased either side of the bay so as to have no effect on the incident wave prior to the run-up of the first wave. For wave angles of 10° and 20°, the run-up in some cases for the wave conditions considered is increased, but not by a significant amount.
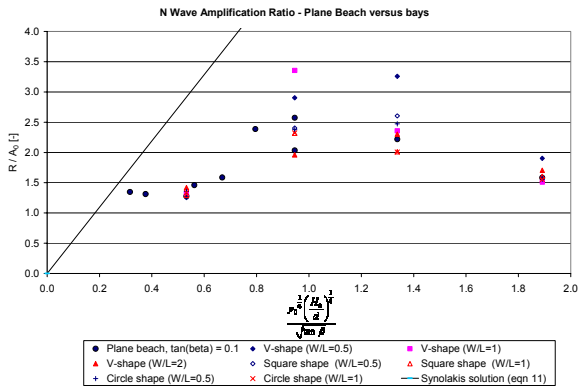
N Wave Amplification Ratio - Plane Beach versus bays

Figure 6. N-wave amplification.

Large bays

Figure 7 illustrates the amplification for sine waves within the large embayments. An opposite frequency response is observed in comparison to the small embayments and plane beaches. Significant amplification, up to a factor six, is observed for V-shaped bays with W/L=0.5 and W/L=1, reducing to a factor 4 for W/L=2. Little amplification is observed for the square bays. The V induces significant amplification at the very landward end of the bay, due to the compression of the wave. This is consistent with the analytical standing wave solution in figure 1. Significant amplification also occurs for shorter wave periods, but this is again limited by breaking. The largest amplification occurs for $\chi \approx 4$. Similar results are found for solitary waves (figure 8) and again maximum amplification occurs at a higher value of the scaling parameter. A breaking criteria given by Synolakis (2003) can be rewritten in terms of the Synolakis scaling parameter adopted previously:

$$\sqrt{\frac{1}{\beta}} \left(p_0 \right)^{\frac{1}{4}} \left(\frac{A}{h_0} \right)^{\frac{1}{4}} > 0.95 \beta^{-\frac{2}{9}} \qquad (7)$$

and appears consistent with the maximum amplification observed in the modelling.

Conclusions

The ANUGA tsunami inundation model has been used to investigate the influence of characteristic coastal morphology on tsunami run-up. For small bays with the water line set close to the entrance to the bay, the V-shape bays increase tsunami run-up by up to 50% for shorter period waves, but have little effect for longer periods. Amplification increases further if the water line is set closer to the apex, up to a factor 2. Maximum amplification occurs for shorter wave periods, which may be expected to break, and appear to do so in the ANUGA model. For large bays, with the water line set at the apex of the bay, an opposite frequency sensitivity is observed. The run-up may be amplified up to six times the incident wave amplitude at the offshore boundary. Breaking can again occur and this results in a complicated amplification pattern.
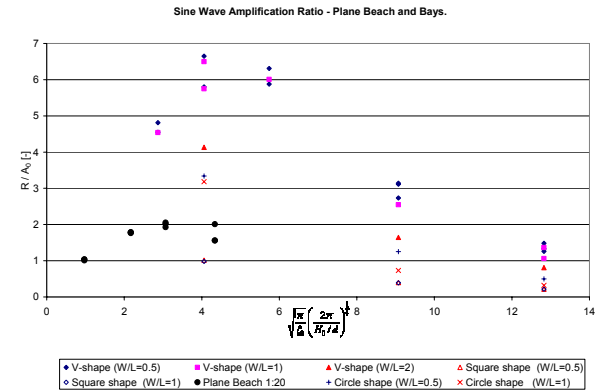
Sine Wave Amplification Ratio - Plane Beach and Bays.

Figure 7. Sine wave amplification, large bays.

Solitary Wave Amplification Ratio - Plane beach and bays
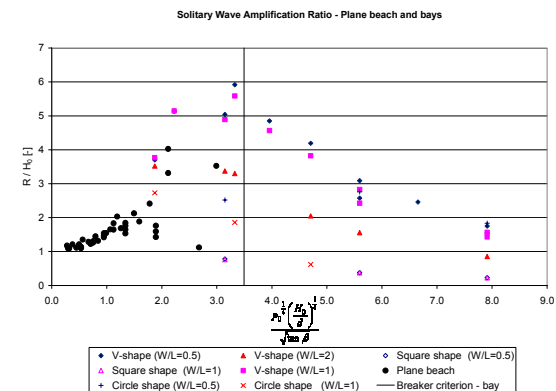
Figure 8. Solitary wave amplification, large bays.

References

[1] Carrier, G.F. and Greenspan, H.P., 1958. *Water waves of finite amplitude on a sloping beach*. J. Fluid Mech., 440: 391-399.

[2] Guard, P. A., Baldock, T. E. and Nielsen, P., 2005. General Solutions for the Initial Run-up of a Breaking Tsunami Front. Int. Symposium on Disaster Reduction on Coasts, University of Melbourne, 14-16 November 2005. CD-ROM.

[3] Keller, J. and Keller, H.B., 1965. *Water wave run-up on a beach*, Part II, Office of Naval Research, Washington D.C., DDC, No. AD0623136.

[4] Lamb, H., 1932. *Hydrodynamics*. 6th Edition. Cambridge University Press.

[5] Nielsen, O., Grey, D., McPherson, A. and Hitchman, A. (2005). *Hydrodynamic modelling of coastal inundation*. Proc. Int. Congress on Modelling and Simulation, 518-523.

[6] Synolakis, C.E., 1987. *The runup of solitary waves*. J. Fluid Mech., 185: 523-545.

[7] Synolakis, C.E., 2003. *Tsunamis and seiches*. In: W.-F.S. Chen, C. (eds) (Editor), Earthquake Engineering Handbook. CRC Press, pp. 9-1 to 9-90.

Acknowledgements